

See discussions, stats, and author profiles for this publication at: <https://www.researchgate.net/publication/233943214>

Preparation and properties of tungsten-doped indium oxide thin films

Article in *Rare Metals* · April 2012

DOI: 10.1007/s12598-012-0483-x

CITATIONS

14

READS

768

4 authors, including:



[Zhang Junying](#)

Beihang University (BUAA)

237 PUBLICATIONS 10,891 CITATIONS

[SEE PROFILE](#)



[Rongming Wang](#)

University of Science and Technology Beijing

354 PUBLICATIONS 15,149 CITATIONS

[SEE PROFILE](#)

Preparation and properties of tungsten-doped indium oxide thin films

LI Yuan, WANG Wenwen, ZHANG Junying, and WANG Rongming

Department of Physics, Beijing University of Aeronautics and Astronautics, Beijing 100191, China

Received 7 July 2011; received in revised form 20 October 2011; accepted 2 November 2011

© The Nonferrous Metals Society of China and Springer-Verlag Berlin Heidelberg 2012

Abstract

Tungsten-doped indium oxide (IWO) thin films were deposited on glass substrate by DC reactive magnetron sputtering. The effects of sputtering power and growth temperature on the structure, surface morphology, optical and electrical properties of IWO thin films were investigated. The thickness and surface morphology of the films are both closely dependent on the sputtering power and the substrate temperature. The transparency of the films decreases with the increase of the sputtering power but is not seriously influenced by substrate temperature. All the IWO thin film samples have high transmittance in near-infrared spectral range. With either the sputtering power or the growth temperature increases, the resistivity of the film decreases at the beginning and increases after the optimum parameters. The as-deposited IWO films with minimum resistivity of $6.4 \times 10^{-4} \Omega\text{-cm}$ were obtained at a growth temperature of 225 °C and sputtering power of 40 W, with carrier mobility of $33.0 \text{ cm}^2\text{-V}^{-1}\text{-s}^{-1}$ and carrier concentration of $2.8 \times 10^{20} \text{ cm}^{-3}$ and the average transmittance of about 81% in near-infrared region and about 87% in visible region.

Keywords: In_2O_3 ; W thin film; DC magnetron sputtering; substrate temperature; sputtering current; optical and electrical properties

1 Introduction

Transparent conducting oxides (TCO) are extensively used in the optoelectronic devices such as in flat panel displays, thin-film solar cells and light emitting diodes [1–3]. Some of the TCO such as tin-doped indium oxide (ITO) and aluminium-doped zinc oxide (AZO) have attracted considerable attention for these applications due to its low electrical resistivity and high transparency in the visible region [4]. It is well known that visible light (400–700 nm) accounts for only 43% of the energy in the solar irradiance spectrum (300–2500 nm), while near-infrared region (NIR, 700–2500 nm) light occupies 52% [5]. However, all commonly used TCO thin films as transparent window electrodes of solar cells have low transparency in the NIR region, limiting the crucial long-wavelength response of solar cells. Therefore, it is necessary to develop a new kind of material to increase the transparency in the NIR region of TCO electrodes.

According to the Drude model [6], high carrier concentration deteriorates the transparency of the TCO films. Therefore, the increase of the transparency window in the NIR range without sacrificing the conductivity can only be obtained by increasing the carrier mobility and keeping relatively low carrier concentration. It is investigated that if Mo^{6+} substitutes for In^{3+} in the In_2O_3 host lattice [7], the va-

lence difference of three between Mo^{6+} and In^{3+} is of great advantage to get high carrier mobility of the $\text{In}_2\text{O}_3\text{:Mo}$ (IMO) films. Just like Mo^{6+} , W^{6+} can also supply three extra electrons when it substitutes In^{3+} [8]. Consequently, tungsten-doped indium oxide (IWO) films have low resistivity with high transparency in the NIR region.

Different techniques such as DC magnetron sputtering [8], radio frequency sputtering [9], electron beam evaporation [10], high density plasma evaporation [11], thermal reactive evaporation [12], spray pyrolysis [13], sol-gel [14], chemical vapor deposition [15], and pulsed laser deposition [16] have been used for deposition of IMO and IWO films. In this paper, polycrystalline IWO thin films were prepared by DC magnetron sputtering using metal target. The effects of sputtering current and substrate temperature on structure, surface morphology, optical and electrical properties of the IWO thin films were investigated.

2 Experimental details

Polycrystalline IWO thin films were deposited on glass substrates by DC magnetron sputtering. The sputtering target made of metal indium (purity: 99.99%) embedded with 6 wt.% metal tungsten (purity: 99.99%) was 64 mm in diameter and 3 mm in thickness. Base pressure of the sputtering

chamber was evacuated to lower than 1×10^{-3} Pa with a turbo molecular pump prior to the deposition period, while pure argon was used as sputtering gas and oxygen as reactive gas. The sputtering parameters maintained during the growth of IWO films are given in Table 1.

Table 1 List of the different deposition parameters

Deposition parameters	Values
Argon flow rate / (ml·min ⁻¹)	38
oxygen flow rate / (ml·min ⁻¹)	12
Sputtering pressure / Pa	1
Sputtering current / mA	100~200
Substrate-target distance / mm	78
Sputtering time / min	5
Substrate temperature / °C	100~375

The crystal structures of the films were analyzed with a Rigaku D/max-2200pc X-ray diffractometer (XRD) using Cu K α radiation, and the diffraction results were recorded in a range of $10 \sim 80^\circ$ (2θ). Scanning electron microscope (SEM) (HITACHIS4200) operating at 20 kV was employed to investigate the morphology of the films. The thickness of the films was determined by Alpha step apparatus (Dektak6M). The optical properties in the wavelength of 300~2500 nm were measured with a spectrophotometer. The Hall mobility and carrier concentration were obtained using Hall-effect measurement by the van der Pauw method.

3 Results and discussion

3.1 Effects of sputtering current on IWO thin films

Figure 1 shows the XRD patterns of IWO films obtained at various sputtering currents while the oxygen partial pressure of 2.4×10^{-1} Pa and sputtering time is 5 min. As shown in this figure, all the diffraction peaks corresponding to the cubic

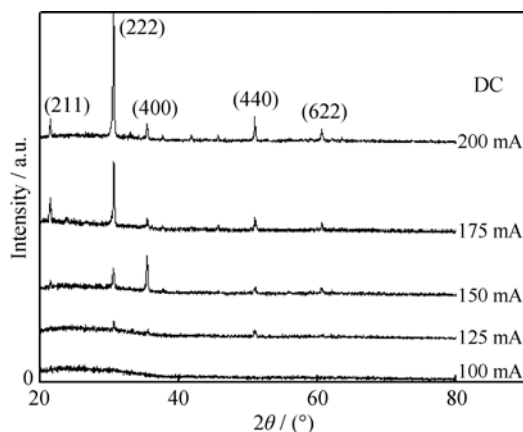


Fig. 1 XRD patterns of IWO films obtained at various sputtering currents

phase of bixbyite-type In_2O_3 can be easily identified and no peaks pertinent to other crystalline structures were observed. It is indicated that the doped tungsten did not change the structure of the In_2O_3 films. Figure 1 also shows that the crystallinity of the IWO films was increased as the sputtering current grew.

Another phenomenon is that with the increase of sputtering current, the preferential orientation of IWO films changes from (400) to (222), which may be caused by insufficient oxidation under high deposition speed, according to our previous study [17]. It is also reported that with high sputtering current, the doped tungsten ion could not be completely oxidized to W^{6+} , and W^{4+} ions also exist [18].

The SEM images of IWO films prepared using different sputtering currents are shown in Fig. 2. The grains deposited on the substrate are dispersedly distributed at low sputtering current. As sputtering current increases, the thickness of the film grows and the distribution of the grains is modified. Regular and compact surface morphology is obtained at 150 mA. However, when the sputtering current further increases, the films are constituted with large size nano-wire monocrySTALLINE and compact structure of the film was broken and the surface roughness increases due to severe insufficiency of oxidation.

The dependences of electrical resistivity, carrier concentration and mobility on the sputtering currents are shown in Fig. 3. It is observed that the resistivity of the film first decreases and then increases after the optimum sputtering current. The as-deposited IWO films with minimum resistivity of $1.9 \times 10^{-3} \Omega\cdot\text{cm}$ are obtained when sputtering current is 150 mA and the sputtering power is 40 W, with carrier mobility of $30 \text{ cm}^2\cdot\text{V}^{-1}\cdot\text{s}^{-1}$ and carrier concentration of $1.1 \times 10^{20} \text{ cm}^{-3}$.

The carrier concentration is found to first increase with an increase in sputtering current under 125 mA and then decrease. At the beginning, with sputtering current increases from 100 to 125 mA, the carrier concentration increases due to the growing of the thickness and the modification of the crystallinity. However, with sputtering current increases from 125 to 200 mA, the carrier concentration decreases, which may be attributed to the incomplete substitution of In ions by doped tungsten ions. The carrier mobility increases with sputtering current increasing from 100 to 150 mA because the crystallinity of the films is modified and compact films are formed during this period. However, the carrier mobility shows a sharp decline when the current grows higher. At high sputtering current, incomplete oxidation will form a large amount of defects and clubbed nano-wire monocrySTALLINES have loose arrangement, resulting in the increase of grain boundary scattering.

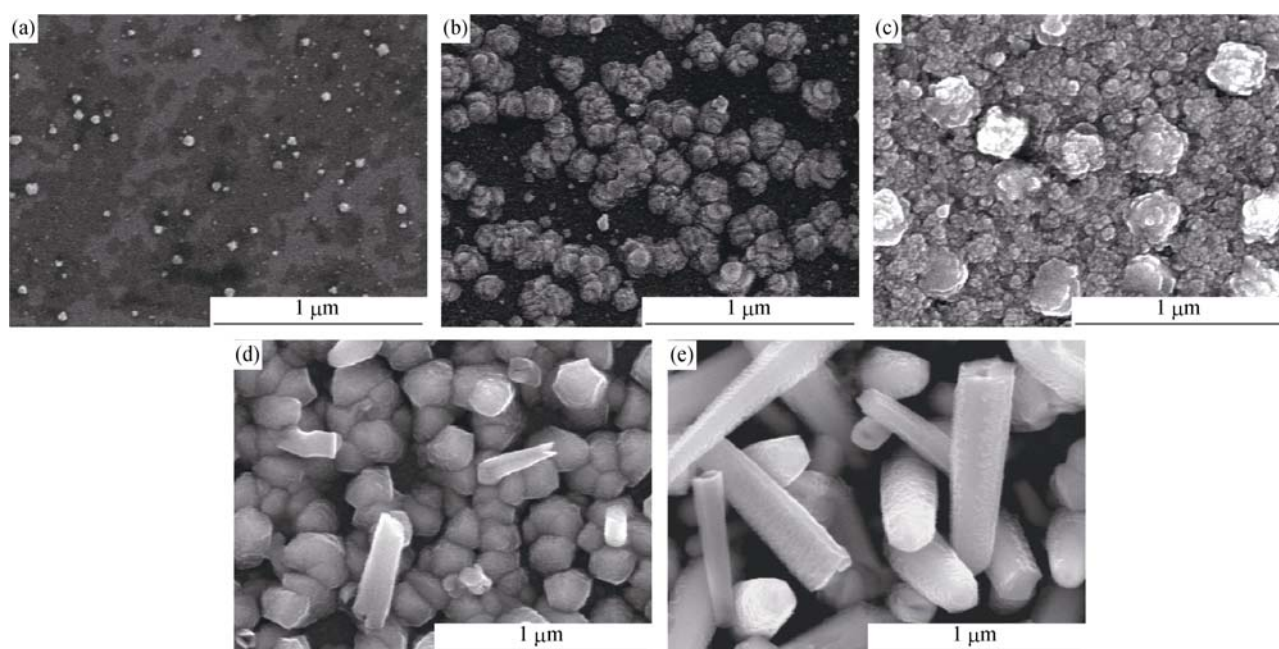


Fig. 2 SEM images of IWO films prepared with different sputtering currents (a) 100 mA; (b) 125 mA; (c) 150 mA; (d) 175 mA; e 200 mA

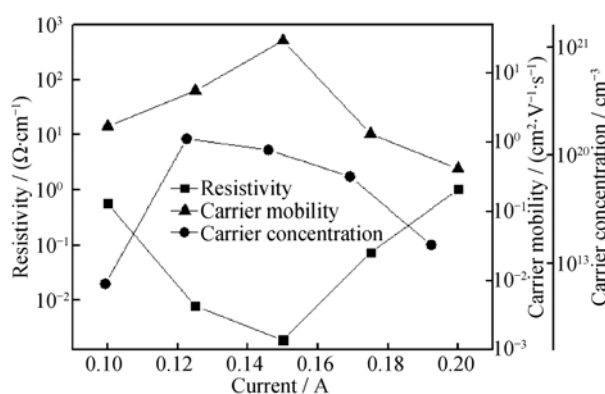


Fig. 3 Effects of sputtering currents on resistivity, carrier concentration and carrier mobility of IWO films

Figure 4 shows the optical transmittance spectra of the IWO films prepared at different sputtering currents in the region of 300–2700 nm. It can be observed that although the transmittances in visible range are diverse, all the IWO samples exhibit high transparency in NIR region. At the same time, the transmittance properties are very sensitive to the sputtering current. The thickness of the films deposited by 100, 125, 150, 175, and 200 mA is 58, 151, 332, 754, and 753 nm, respectively. It's reasonable that the transparency of the films decreases with the increase of the thickness. Although the thickness of the IWO film obtained at 200 mA is thinner than that at 150 mA, the transparency of the former is the lowest because of the higher surface roughness than the latter.

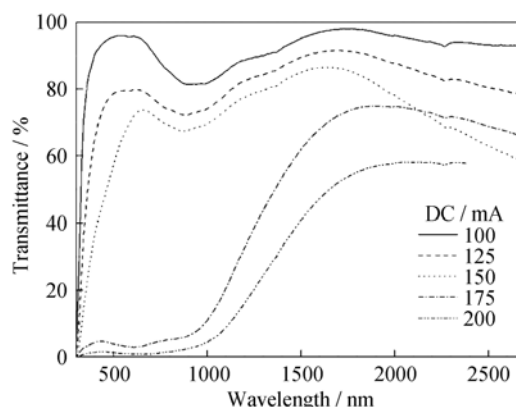


Fig. 4 Optical transmittance spectra of the IWO films prepared at different sputtering currents in the region of 300–2700 nm

3.2 Effects of substrate temperature on IWO thin films

The effects of substrate temperature on the XRD patterns of IWO thin films are shown in Fig. 5. These films were deposited at different temperatures when the oxygen partial pressure and sputtering current are kept at 2.4×10^{-1} Pa and sputtering current 150 mA, respectively. As shown in this figure, all peak positions are in good agreement with the cubic phase of bixbyite-type In_2O_3 . The crystallinity of the films is modified with substrate temperature increasing from 100 to 375 °C. The average particle size of the films was calculated using the Scherrer equation [19], and the results show that the particle size of the film is not seriously influenced by the substrate temperature.

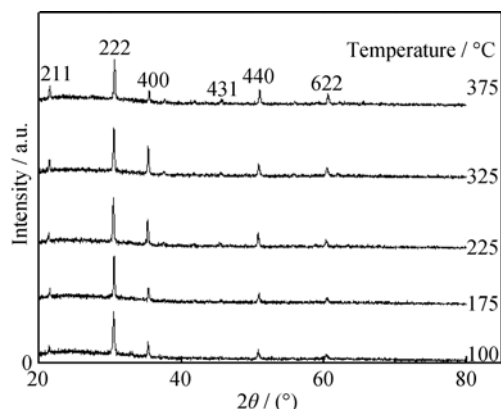


Fig. 5 XRD patterns of IWO films prepared at different substrate temperatures

Figure 6 shows the SEM images of IWO films prepared at different substrate temperatures. It seems the surface morphology in the film consisted of the grains and uniform plane. However, we investigate the $1\ \mu\text{m}$ SEM images of IWO films; the uniform plane also consisted of the smaller grains actually. This phenomenon has not been found in other references. As the substrate temperature increases from 100 to 325 °C, the grain size of the films grows slightly, which are 128, 194, 216, 270, and 1068 nm, respectively. The grain sizes of all the samples appear to be very uniform due to the formation of a solid solution. The surface migration energy and the nucleation quantity are both increased with the increase of substrate temperature, resulting in the compact and smooth surface of the film when the

temperature reaches 325 °C. The IWO film obtained at 375 °C has much larger and longer grains on the surface, which may be caused by the high diffusion rate of the sputtered atoms on the substrate [20].

The effect of substrate temperature on electrical properties of IWO films is shown in Fig. 7. The relationships of resistivity, carrier concentration and carrier mobility of IWO films with the substrate temperature were investigated. It is observed from Fig. 7 that the resistivity initially decreases with the increase of the substrate temperature and reaches a minimum value of $6.4 \times 10^{-4}\ \Omega\cdot\text{cm}$ at 225 °C. After that, the resistivity is increased by further increase of the substrate temperature. It is found that both carrier concentration and carrier mobility reach the optimum values at 225 °C, and start to decrease upon further substrate temperature increasing. The initial increase in carrier concentration depends on the improvement of the crystallinity, which leads to decreases in capture traps and grain boundary scattering [20]. The carrier concentration decreases when the temperature increases higher than 225 °C, because that better crystallinity causes the extinction of oxygen vacancies of the film [21]. Generally, the carrier mobility is influenced by several scattering mechanisms including lattice, neutral impurity, ionized impurity and grain boundary scattering [22]. The influence of lattice vibration scattering and neutral impurity scattering on highly degenerated films at room temperature can be ignored [18]. Therefore, the mobility of IWO films is found to be mainly limited by the ionized impurity and grain

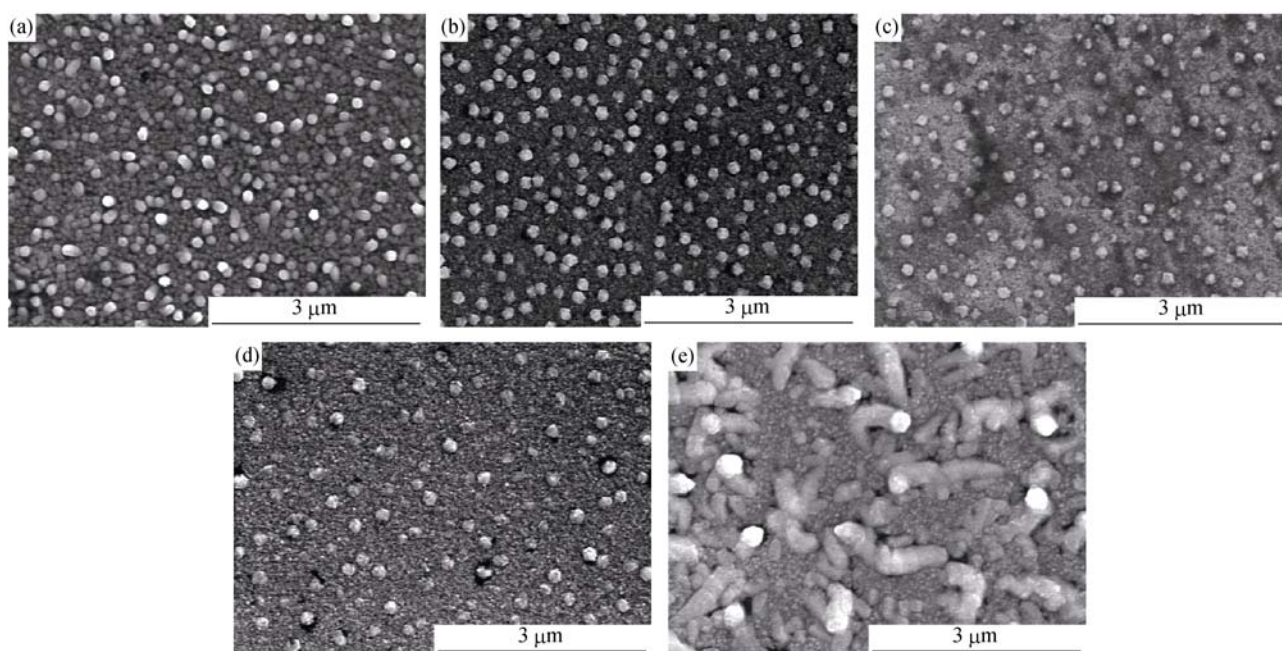


Fig. 6 SEM images of IWO films deposited at different substrate temperatures (a) 100 °C; (b) 175 °C; (c) 225 °C; (d) 325 °C; (e) 375 °C

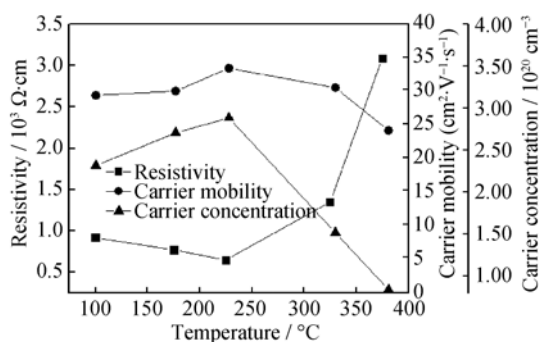


Fig. 7 Dependences of electrical resistivity, carrier concentration and mobility of IWO films on substrate temperature

boundary scattering. When the substrate temperature increases from 100 to 225 °C, the carrier mobility increases due to the decrease in grain boundary scattering caused by the improvement of the crystallinity. When the temperature grows higher, the carrier mobility decreases because of the loose arrangement of the large crystalline grains.

Figure 8 shows the effect of substrate temperature on optical transmittance of IWO films in the range of 300–2700 nm. It is found that the transparency of the films is not seriously influenced by the substrate temperature. The film deposited at 100 °C has the lowest optical transparency, and the optical transmittance increases with the increase of the deposited temperature, because the crystallinity of the films is modified and compact surface is obtained. In visible range, the optical transmittance of the film deposited at 375 °C declines slightly, which could be attributed to the irregular arrangement of the large and long grains on the surface, as shown in the surface morphology picture. The long and irregular arranged grains result in a rough surface of the sample, which increases the diffuse reflection of the film. Therefore, the optical transmittance of the film declines.

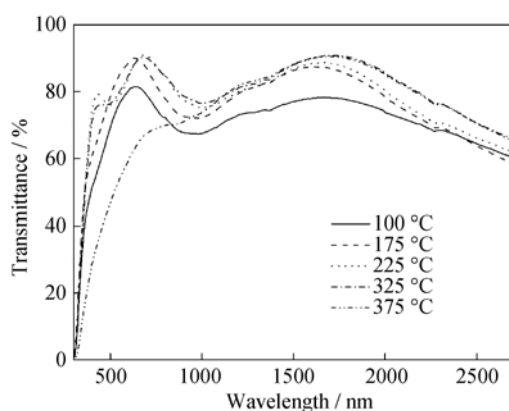


Fig. 8 Optical transmittance spectra of the IWO films deposited at different substrate temperatures in the region of 300–2700 nm

4 Conclusion

Highly conducting tungsten-doped indium oxide (IWO) thin films with high transparency in NIR region were deposited on glass substrates using metallic targets by DC reactive magnetron sputtering. These films are highly oriented along (222) direction with smooth and compact surface morphology. The electrical properties of the films depend both on sputtering current and substrate temperature. The transparency of the film apparently decreases with the increase of the sputtering power but is not seriously influenced by the changing of the substrate temperature. IWO film with the highest carrier mobility of $33 \text{ cm}^2 \cdot \text{V}^{-1} \cdot \text{s}^{-1}$, carrier concentration of $2.8 \times 10^{20} \text{ cm}^{-3}$, and a relatively low resistivity of $6.4 \times 10^{-4} \Omega \cdot \text{cm}$ was obtained at a growth temperature of 225 °C and sputtering power of 40 W. At the same time, the average transmittance of the film is about 81% in NIR region and 87% in visible region.

Acknowledgments

This work was supported by the National Natural Science Foundation of China (No. 50902006) and the National High Technology Development 863 Program of China (No. 2009AA03Z428).

References

- [1] Carvalho C.N., Lavareda G., Amaral A., Conde O., and Ramos A.R., InO_x semiconductor films deposited on glass substrates for transparent electronics, *J. Non-Cryst. Solids*, 2006, **352** (23-25): 2315.
- [2] Selvan J.A.A., Delahoy A.E., Guo S., and Li Y. M., A new light trapping TCO for nc-Si:H solar cells, *J. Sol. Energy Mater. Sol. Cells*, 2006, **90** (18-19): 3371.
- [3] Silva V.M., and Pereira L., The nature of the electrical conduction and light emitting efficiency in organic semiconductor layers: the case of [m-MTDATA] – [NPB] – Alq3 OLED, *J. Non-Cryst. Solids*, 2006, **352** (50-51): 5429.
- [4] Szyszka B., Sittinger V., Jiang X., Hong R.J., Werner W., Pflug A., Ruske M., and Lopp A., Transparent and conductive ZnO:Al films deposited by large area reactive magnetron sputtering, *J. Thin Solid Films*, 2003, **442** (1-2): 179.
- [5] Levinson R., Berdahl P., and Akbari H., Solar spectral optical properties of pigments—Part II: survey of common colorants, *J. Sol. Energy Mater. Sol. Cells*, 2005, **89** (4): 351.
- [6] Hamberg I., and Granqvist C.G., Evaporated Sn-doped In_2O_3 films: basic optical properties and applications to energy-efficient windows, *J. Appl Phys*, 1986, **60** (11): 123.
- [7] Yoshida Y., Gessert T.A., Perkins C.L., and Coutts T.J., Development of radio-frequency magnetron sputtered indium

- molybdenum oxide, *J. Vac. Sci. Technol.*, 2003, **21** (4): 1092.
- [8] Miao W., Li X.F., Zhang Q., Huang L., Zhang Z., Zhang L., and Yan X., Transparent conductive $\text{In}_2\text{O}_3\text{:Mo}$ thin films prepared by reactive direct current magnetron sputtering at room temperature, *J. Thin Solid Films*, 2006, **500** (1-2): 70.
- [9] Xiu X.W., Pang Z.Y., Lü M., Dai Y., Ye L., and Han S., Transparent conducting molybdenum-doped zinc oxide films deposited by RF magnetron sputtering, *J. Appl. Surf. Sci.*, 2007, **253** (6): 3345.
- [10] Hjortsberg A., Hamberg I., and Granqvist C.G., Transparent and heat-reflecting indium tin oxide films prepared by reactive electron beam evaporation, *J. Thin Solid Films*, 1982, **90** (3): 323.
- [11] Sun S.Y., Huang J., and Lii D.F., Effects of oxygen contents on the electrical and optical properties of indium molybdenum oxide films fabricated by high density plasma evaporation, *J. Vac. Sci. Technol.*, 2004, **22** (4): 1235.
- [12] Nath Prem, Bunshah R.F., Basol B.M., and Staffsud O.M., Electrical and optical properties of $\text{In}_2\text{O}_3\text{:Sn}$ films prepared by activated reactive evaporation, *J. Thin Solid Films*, 1980, **72** (3): 463.
- [13] Bian J.M., Li X.M., Gao X.D., Yu W.D., and Chen L.D., Deposition and electrical properties of N-In codoped p-type ZnO films by ultrasonic spray pyrolysis, *J. Applied Physics Letters*, 2004, **84** (4): 3.
- [14] Wang H., Tang Z.Y., Sun L., He Y.B., Wu Y.X., and Li Z.Y., Novel electrode materials for thin-film ultracapacitors: capacitance performance enhancement of TiO_2 doped with Ni and graphite, *Rare Metals*, 2009, **28** (3): 231.
- [15] Hu J.H., and Gordon R.G., Textured aluminum-doped zinc oxide thin films from atmospheric pressure chemical-vapor deposition, *J. Appl. Phys.*, 1992, **71** (2): 880.
- [16] Gupta R.K., Ghosh K., and Kahol P.K., Thickness dependence of optoelectrical properties of tungsten-doped indium oxide films, *J. Appl. Surf. Sci.*, 2009, **255** (21): 8926.
- [17] Li Y., Wang W.W., and Zhang J.Y., Fabrication and photoelectric properties of tungsten-doped indium oxide films, *Journal of Functional Materials*, 2011, **1** (8): 1457. (In Chinese)
- [18] Li X.F., Zhang Q., and Miao W.N., Transparent conductive oxide thin films of tungsten-doped indium oxide, *J. Thin Solid Films*, 2006, **515** (4): 2471.
- [19] Zhang W.W., Zhang J.Y., Li Y., and Chen Z.Y., Preparation and optical properties of $\text{ZnGa}_2\text{O}_4\text{:Cr}^{3+}$ thin films derived by sol-gel process, *J. Applied Surface Science*, 2010, **256** (14): 4702.
- [20] Jiang X., Sun C., and Hong R.J., *Transparent Conductive Oxides Films*, Beijing: Higher Education Press, 2008: 57-69, 159, 210, 233-241, 205-207, 278.
- [21] Liu Y.D., and Lian J.S., Optical and electrical properties of aluminum-doped ZnO thin films grown by pulsed laser deposition, *J. Applied Surface Science*, 2007, **253** (7): 3727.
- [22] Pei Z.L., Sun C., Tan M.H., Xiao J.Q., Guan D.H., Huang R.F., and Wen L.S., Optical and electrical properties of direct-current magnetron sputtered ZnO:Al films, *J. Appl. Phys.*, 2001, **90** (7): 3432.